

**Cell Reports, Volume 15**

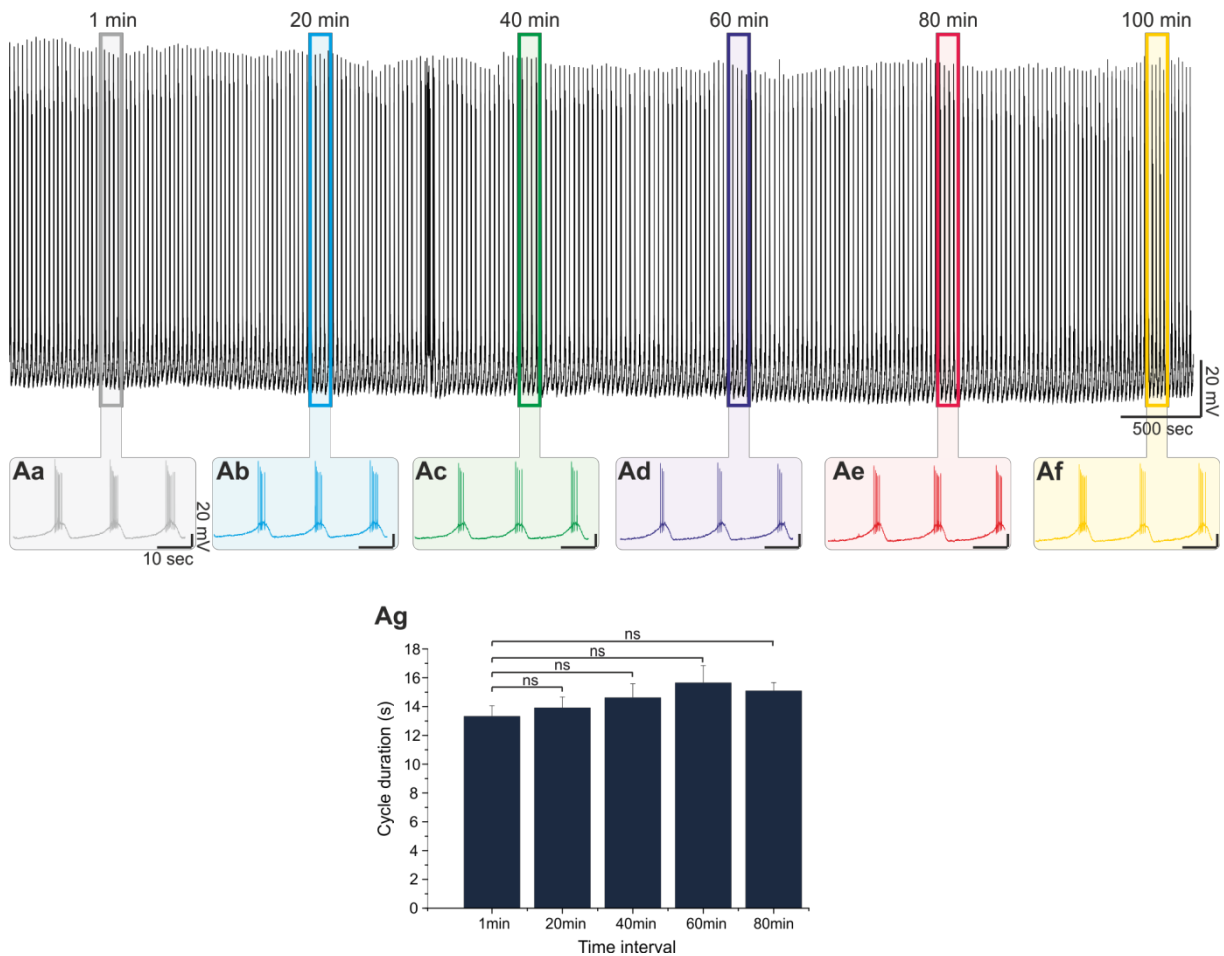
**Supplemental Information**

**Dopamine Autoreceptor Regulation  
of a Hypothalamic Dopaminergic Network**

**Stefanos Stagkourakis, Hoseok Kim, David J. Lyons, and Christian Broberger**

1 SUPPLEMENTAL INFORMATION

2



3

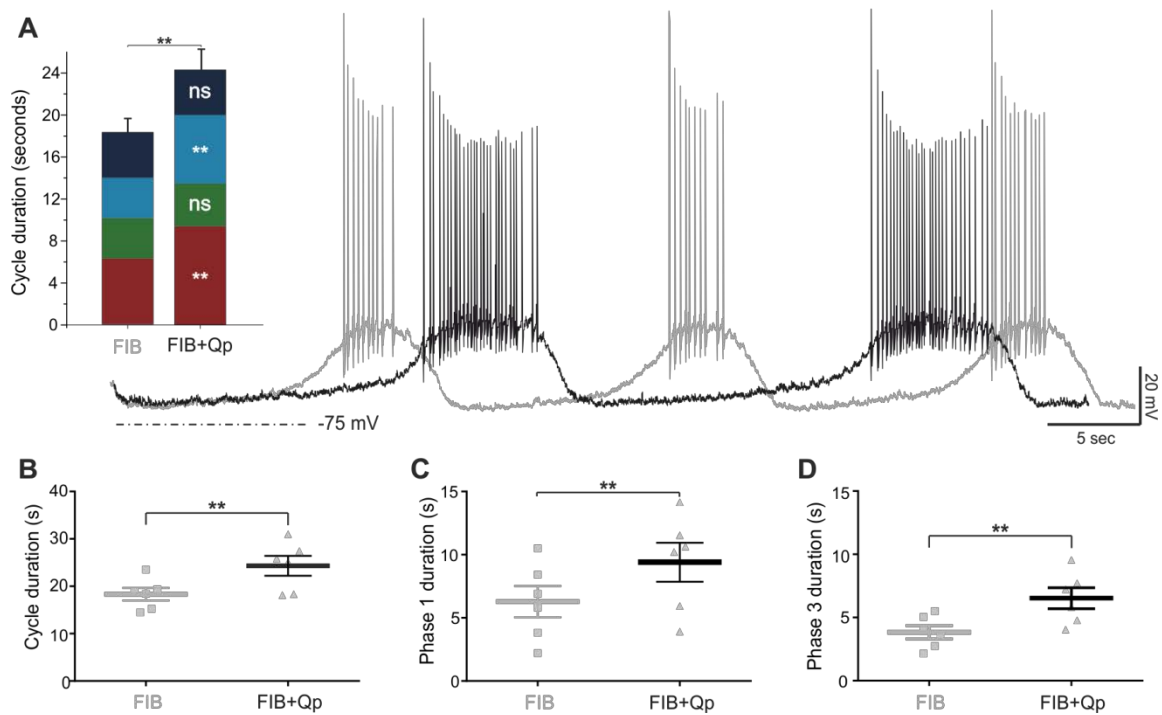
4 **Figure S1. Robustness of the TIDA oscillation and maintenance of rhythmicity in long whole-cell**  
5 **recordings, see Experimental Procedures.**

6 (Aa-g) Cycle duration does not change in control long-term recordings ( $+0.71 \pm 0.55$  s;  $p > 0.05$  at  $t=40$  min vs  $t=1$   
7 min;  $n=6$ ). (Ag) Cycle duration does not change in control long-term recordings in an 80 min period ( $+0.97 \pm 1.03$   
8 s;  $p > 0.05$  at  $t=80$  min vs  $t=1$  min;  $n=3$ ).

9

10

11

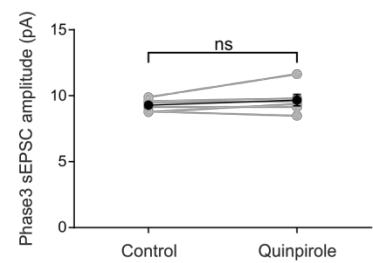
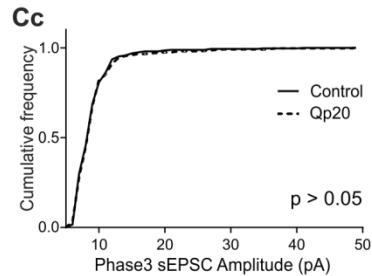
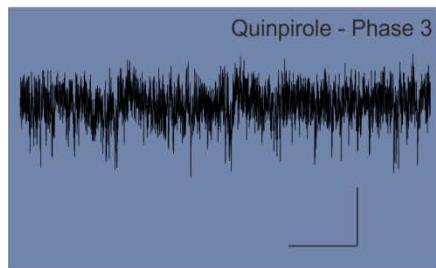
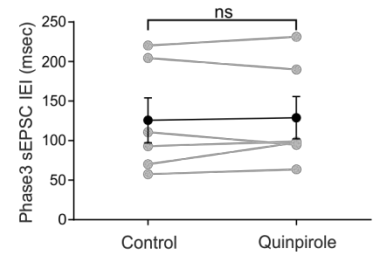
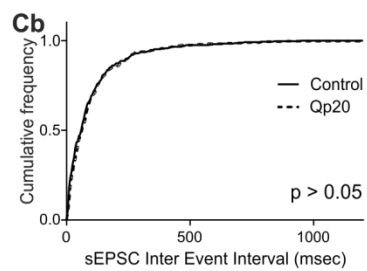
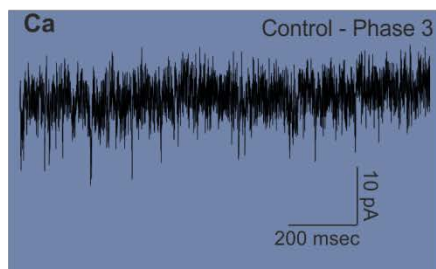
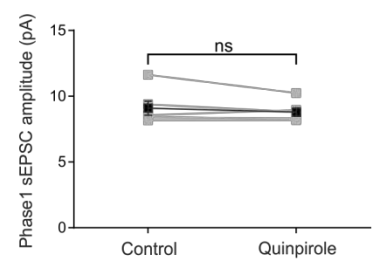
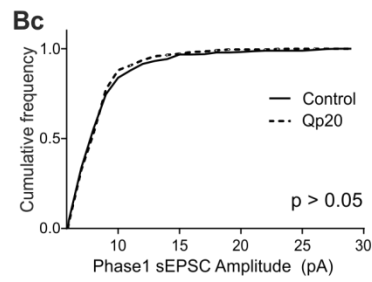
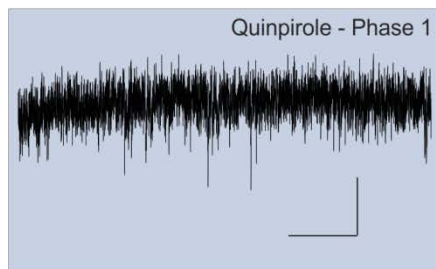
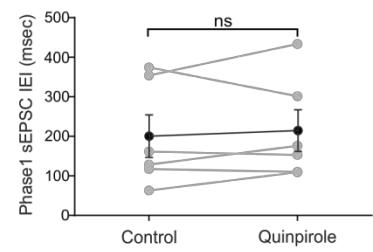
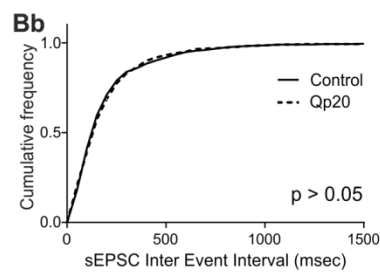
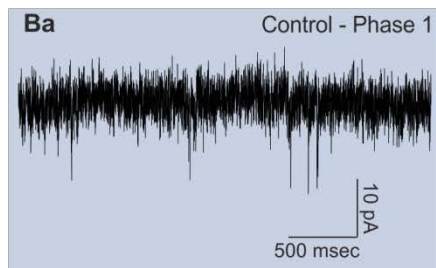
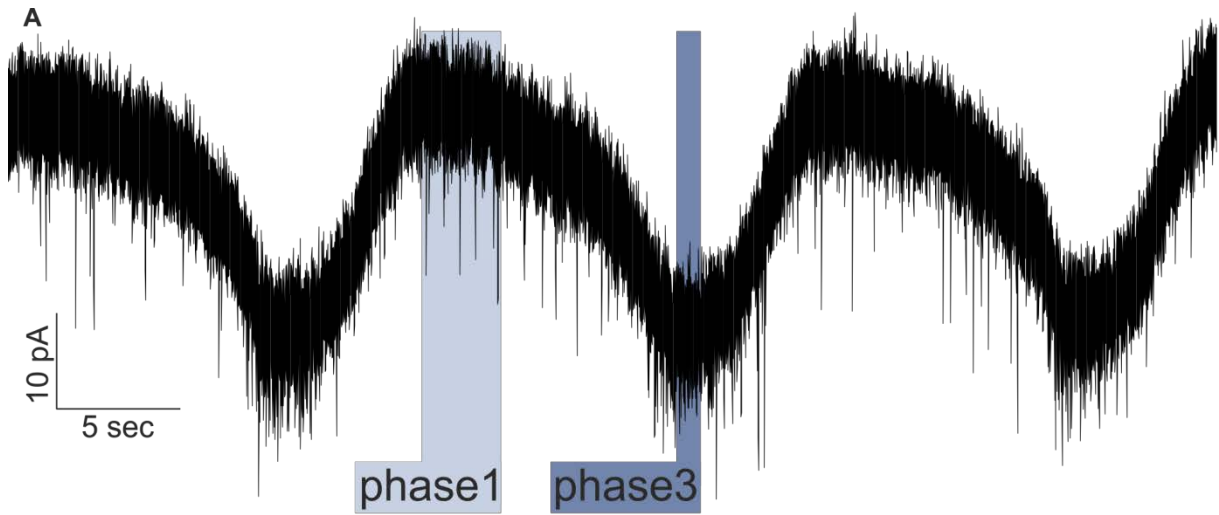


12

13 **Figure S2. Related to Figure 1; D2R activation effect on cycle and phase duration persists in fast**  
 14 **ionotropic blockade.**

15 (A) Quinpirole application leads to an increase in cycle duration in the presence of fast ionotropic blockade (FIB;  
 16 Picrotoxin 100  $\mu$ M, CNQX 10  $\mu$ M and AP-5 25  $\mu$ M) via phase 1 and phase 3 prolongation. (B) Cycle duration  
 17 increase ( $+5.99 \pm 0.91$  s;  $p < 0.01$  vs FIB;  $n=6$ ). (C) Phase 1 duration increase ( $+3.12 \pm 0.52$  s;  $p < 0.01$  vs FIB;  $n=6$ ).  
 18 (D) Phase 3 duration increase ( $+2.69 \pm 0.47$  s;  $p < 0.01$  vs FIB;  $n=6$ ).

19



20

21

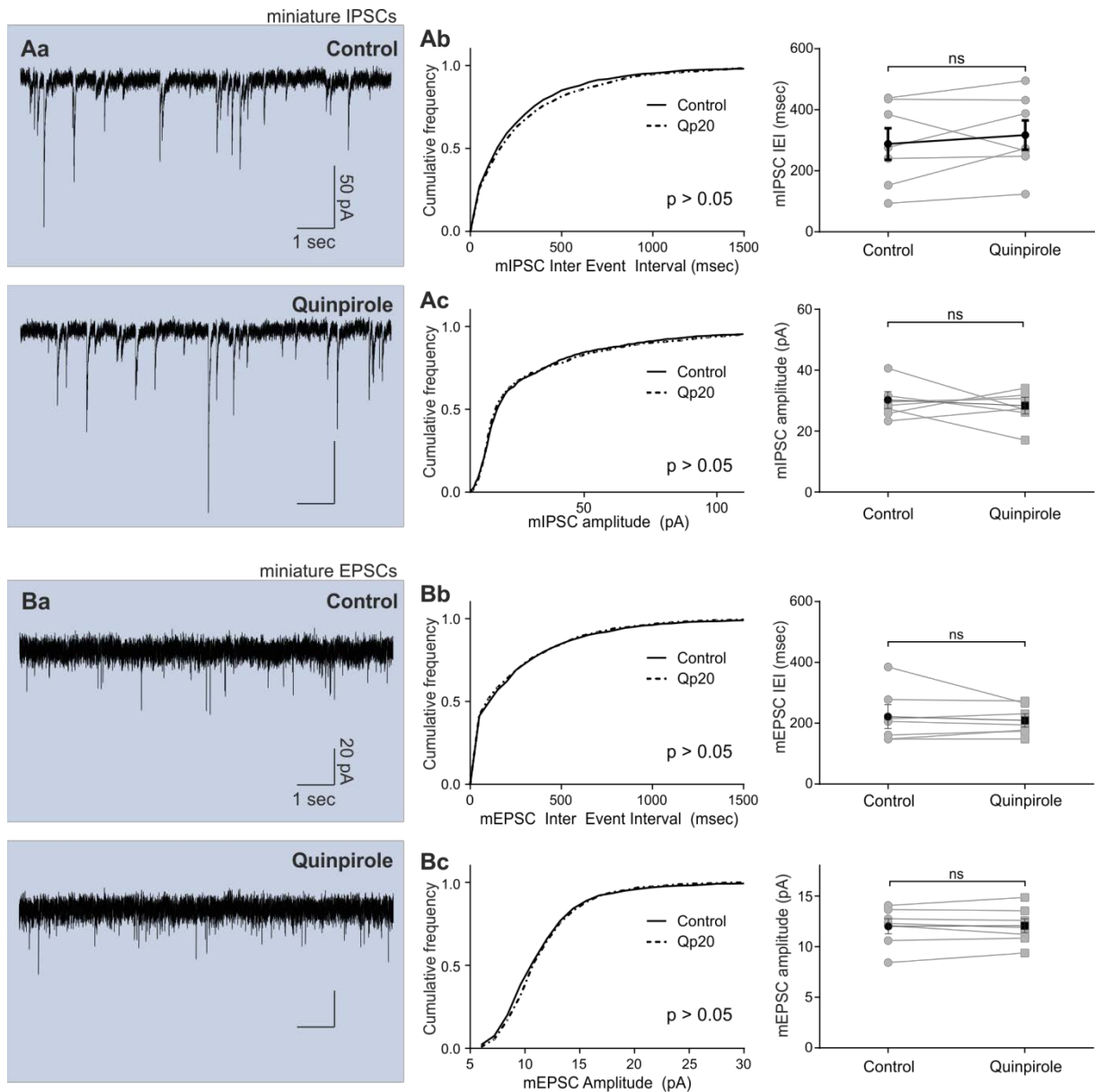
22

23 **Figure S3. Related to Figure 5; Spontaneous EPSCs are not affected by D2R activation.**

24 (Aa) Raw voltage clamp trace demonstrating the time intervals from which sEPSCs were sampled during phase  
25 1 (light blue) and phase 3 (dark blue). (Ba) Raw voltage clamp traces in control vs quinpirole illustrating no  
26 change in sEPSC frequency or amplitude during phase 1. (Bb) Cumulative frequency distribution of sEPSC  
27 inter-event interval demonstrating no difference in frequency ( $+14.18 \pm 22.30$  ms, KS-2  $p < 0.05$ ;  $t$ -test  $p < 0.05$ ;  
28  $n=5$ ) or amplitude (Bc) ( $-0.29 \pm 0.25$  pA, KS-2  $p > 0.05$ ;  $t$ -test  $p > 0.05$ ;  $n=5$ ) during phase 1. (Ca) Raw voltage  
29 clamp trace illustrating no difference in frequency or amplitude of sEPSCs during phase 3 after quinpirole  
30 application. (Cb) Cumulative frequency distribution of sEPSC inter event interval demonstrating no difference in  
31 frequency ( $+3.28 \pm 6.73$  ms, KS-2  $p < 0.05$ ;  $t$ -test  $p < 0.05$ ;  $n=5$ ) or amplitude (Cc) ( $+0.38 \pm 0.30$  pA, KS-2  $p > 0.05$ ;  $t$ -  
32 test  $p > 0.05$ ;  $n=5$ ) during phase 3.

33

34



35

36 **FigureS4. Related to Figure 5; Miniature synaptic transmission is unaffected by D2R activation in TIDA**  
 37 **neurons.**

38 (Aa) Raw voltage clamp traces in control vs quinpirole illustrating no change in miniature IPSC frequency or  
 39 amplitude. (Ab) Cumulative frequency distribution of mIPSC inter-event interval demonstrating no difference in  
 40 frequency ( $+29.07 \pm 30.56$  ms, KS-2  $p < 0.05$ ;  $t$ -test  $p < 0.05$ ;  $n = 7$ ) or amplitude (Ac) ( $-1.78 \pm 3.07$  pA, KS-2  $p > 0.05$ ;  
 41  $t$ -test  $p > 0.05$ ;  $n = 7$ ). (Ba) Raw voltage clamp trace illustrating no difference in frequency or amplitude of  
 42 mEPSCs as a result of quinpirole application. (Bb) Cumulative frequency distribution of mEPSC inter-event  
 43 interval demonstrating no difference in frequency ( $-10.75 \pm 18.73$  ms, KS-2  $p < 0.05$ ;  $t$ -test  $p < 0.05$ ;  $n = 7$ ) or (Bc)  
 44 amplitude ( $+0.06 \pm 0.24$  pA, KS-2  $p > 0.05$ ;  $t$ -test  $p > 0.05$ ;  $n = 7$ ).

45

46

**Table S2. Related to Figure 2 Ac-Ad and Bc-Bd; D2R antagonists decrease the amplitude and broaden the TIDA action potentials.**

		Control	Eticlopride 1 $\mu$ M
Amplitude (mV)	AP1	97.41 $\pm$ 1.12	85.83 $\pm$ 2.05 **
	AP2	85.87 $\pm$ 1.79	71.77 $\pm$ 2.19 **
	AP3	79.74 $\pm$ 1.43	61.55 $\pm$ 3.86 **
	AP4	75.35 $\pm$ 1.65	57.79 $\pm$ 3.36 **
	AP5	72.35 $\pm$ 1.54	54.34 $\pm$ 3.01 **
Half-width (ms)	AP1	1.49 $\pm$ 0.10	1.56 $\pm$ 0.09
	AP2	1.74 $\pm$ 0.14	1.93 $\pm$ 0.14 **
	AP3	1.91 $\pm$ 0.16	2.36 $\pm$ 0.26 *
	AP4	2.08 $\pm$ 0.18	2.54 $\pm$ 0.25 **
	AP5	2.17 $\pm$ 0.18	2.79 $\pm$ 0.39 *
		Control	Haloperidol 1 $\mu$ M
Amplitude (mV)	AP1	95.09 $\pm$ 1.91	89.11 $\pm$ 2.26 **
	AP2	85.00 $\pm$ 2.28	76.82 $\pm$ 2.76 **
	AP3	79.73 $\pm$ 2.93	68.85 $\pm$ 2.94 ***
	AP4	74.38 $\pm$ 2.25	63.95 $\pm$ 2.77 **
	AP5	74.16 $\pm$ 2.44	59.28 $\pm$ 2.13 **
Half-width (ms)	AP1	1.37 $\pm$ 0.02	1.41 $\pm$ 0.04
	AP2	1.53 $\pm$ 0.04	1.63 $\pm$ 0.04 *
	AP3	1.67 $\pm$ 0.06	1.82 $\pm$ 0.05 **
	AP4	1.79 $\pm$ 0.06	1.97 $\pm$ 0.07 **
	AP5	1.82 $\pm$ 0.07	2.14 $\pm$ 0.07 **

47

48

49 **SUPPLEMENTAL EXPERIMENTAL PROCEDURES**

50 *Ca<sup>2+</sup> current studies.* To examine modulation of Ca<sup>2+</sup> channels, bath application of TTX (0.5μM) was used to  
51 block the voltage-gated Na<sup>+</sup> conductance (Cohen et al., 1981) and Ba<sup>2+</sup> (1mM) was added to the extracellular  
52 solution to augment the Ca<sup>2+</sup> channel currents (Kostiuk et al., 1985, Smith et al., 1986). The Cs<sup>+</sup>-based  
53 intracellular solution described for recordings of EPSCs (see above) was used to block K<sup>+</sup> currents (Adelman and  
54 Senft, 1966, Clay and Shlesinger, 1984). At the end of every experiment CdCl<sub>2</sub> (400 μM) was applied to abolish  
55 the Ca<sup>2+</sup> conductances (Thevenod and Jones, 1992, Swandulla and Armstrong, 1989); that recording was used as  
56 the negative control. Due to incomplete blockade of the K<sup>+</sup> leak conductance by Cs<sup>+</sup>, the Cd<sup>2+</sup> trace was  
57 subtracted digitally from Ca<sup>2+</sup> recordings of the same neuron. Run-down of Ca<sup>2+</sup> currents was minimized by  
58 using the Cs<sup>+</sup>-based intracellular solution (Zhang et al., 1994), by applying brief (150 ms) ramp protocols  
59 adapted from (Chen and Kirchgeßner, 2002), and by waiting for 10 mins between activating currents, a time  
60 interval that was used for pharmacological reagents to reach a peak of effect. In these conditions, run-down of  
61 the HVA Ca<sup>2+</sup> current was calculated to be 3.3±0.69% per 10 min (n=3). The values of all Ca<sup>2+</sup> peak currents  
62 were corrected based on the run-down estimate.

63

64 *Oscillation phase analysis.* We developed a Matlab script in order to isolate the contribution of each phase to the  
65 oscillation cycle duration. The stereotyped traits of the oscillation were used to develop an algorithm, to allow  
66 analysis of duration and membrane voltage of the four phases of the duty cycle. Four phases were defined on the  
67 basis of slope (dV/dt) changes (Figure 1A): Phase 1 was defined as the slow depolarizing phase beginning at the  
68 nadir of the membrane potential (the lowest mV value of an oscillation cycle) and ending within a time window  
69 of 0.5-4sec prior to the first action potential of the oscillation cycle, where the point of maximal change in slope  
70 defines the phase 2 initiation point. Phase 2 was thus defined as the fast depolarizing phase beginning at the  
71 phase 2 initiation point and ending at the firing threshold (defined as dV/dt>5 mV/ms) of the first action  
72 potential of the oscillation cycle. Phase 3 was defined as the action potential firing plateau phase, extending  
73 between the firing threshold of the first action potential of the oscillation cycle until the end of firing where the  
74 maximal change in slope defines the end of phase 3 and beginning of phase 4. Phase 4 constitutes the fast  
75 hyperpolarizing phase between end of phase 3 and the ensuing nadir point.

76 *Recording of EPSCs and IPSCs.* In recordings of sIPSCs and mIPSCs whole-cell voltage-clamp recordings were  
77 performed with micropipettes filled with intracellular solution containing (in mM), 150 KCl, 10 HEPES, 10  
78 EGTA, and 2 Na<sub>2</sub>ATP, pH 7.3 (with KOH), in the presence of fast excitatory neurotransmission blockade by  
79 CNQX (10 μM) and AP-5 (25 μM). The final part of every s/mIPSCs recording was application of picrotoxin  
80 (100 μM) and the observation of complete loss of all synaptic events. In recordings of sEPSCs and mEPSCs  
81 whole-cell voltage-clamp recordings were performed with micropipettes filled with intracellular solution  
82 containing (in mM), 140 K-gluconate, 10 KCl, 10 HEPES, 10 EGTA, and 2 Na<sub>2</sub>ATP, pH 7.3 (with KOH), in the  
83 presence of fast inhibitory neurotransmission blockade by picrotoxin (100 μM). The final part of every  
84 s/mEPSCs recording was application of picrotoxin (100 μM) and the observation of complete loss of all synaptic  
85 events. sIPSCs and sEPSCs along phases were compared via manual selection. Beginning of phase 1 in voltage-  
86 clamp was defined as the most positive point (in pA), of a new oscillation cycle and beginning of phase 3 was  
87 selected as the most negative point (in pA) of the oscillation cycle.



88 *Reagents.* Dopamine hydrochloride, apomorphine hydrochloride hydrate, picrotoxin, cadmium chloride,  
89 haloperidol, BaCl<sub>2</sub> and (TEA)-Cl<sub>2</sub> were purchased from Sigma. TTX and charybdotoxin were purchased from  
90 Alomone Labs. (-)-quinpirole hydrochloride, SKF-81297 hydrobromide, (-)-Eticlopride hydrochloride, CNQX,  
91 AP-5, nimodipine and CGP 55845 hydrochloride were purchased from Tocris Bioscience. GVIA ω-conotoxin  
92 was purchased from Abcam biochemical.

93